

# Machinability analysis of carbon fibre-reinforced plastics (CFRP) using compression tools

Balázs SOMOSKŐI, Norbert GEIER

Budapest University of Technology and Economics, Department of Manufacturing Science and Engineering  
Műegyetem rkp. 3., 1111 Budapest, Hungary  
somibali@gmail.com, geier@manuf.bme.hu

**Abstract** — The widely spread use of polymer composites and their difficult machining behaviour have directly led to the appearance of tools with unique geometry, specialised for carbon fibre-reinforced plastics (CFRP). These so called compression tools are crafted in a way to reduce delamination, which is a common machining caused material defect. The present study focuses on the effect of technological factors on various optimization parameters in cases compression tools were used. Cutting width and feed rate have been chosen as factors. The factor levels have been determined beforehand, using central composite inscribed (CCI) design. The machining experiments were carried out on a Kondia B640 milling machine centre. A KISTLER 9257BA load cell was used for the measurement of the cutting force, likewise a Mahr Federal Pocket Surf IV instrument for surface roughness. Collected data were processed using analysis of variance (ANOVA) and response surface methodology (RSM) via Minitab 17. As a result of this research the change of tool-geometry and process parameters of CFRP machining were determined, induced by technological parameters, on two various compression tools. It was found that the feed rate has the most significant effect on the cutting force and surface roughness, followed by the cutting width.

**Keywords** — CFRP; milling; compression tool; multitooth tool; cutting force; surface roughness

## 1 INTRODUCTION

Lately widespread of carbon fibre-reinforced plastics (CFRP) was caused by its outstandingly high specific strength and specific modulus [1], [2]. Nowadays, composites are widely used in military-, automotive- and aviation industry. Aircraft constructions such as a Boeing 787 consist composites up to 50% by weight and 70% by volume [3]. Manufacturers aim to mold CFRP parts, to match their final size and shape. Moreover they use force bounded and glued joinings [4], [5]. However machining of these components is inevitable to meet required tolerances, and in some cases the final desired shape [6]. There have been preliminary studies on the milling of CFRP in order to optimize milling parameters. Geier et al. [7] have determined that the feed rate is the most significant parameter when it comes to cutting force. They also stated that the increase of feed rate results in the growth of cutting force. Wang et al. [8] have also verified this statement, and also concluded, that the next most determinative factor during face milling is the cutting width. In their paper they stated that parameter's raise also causes the increase of cutting force. One of the most systematic studies on surface roughness optimization was conducted by Khairurshima et al. [9]. In their analysis they found that the most

important factor in this aspect of research is the feed rate. Furthermore, at a constant feed rate surface roughness is the lowest, when the lowest cutting width is applied. Although all these previous studies, CFRP specific tools have been rarely researched.

### 1.1 Compression tools

Compression tools (in some papers also called multitooth tools) are crafted specifically for the milling of CFRP. These tools are fabricated with a geometry, which directs passiv force components towards the center of the layers, thus pressing them together. This mechanism is favorable to avoid delamination (separation of layers in the composite material). Tool manufacturers reach this effect for instance with the formation of a double opposed helix along the tool's cyclinder surface, represented on Fig. 1.

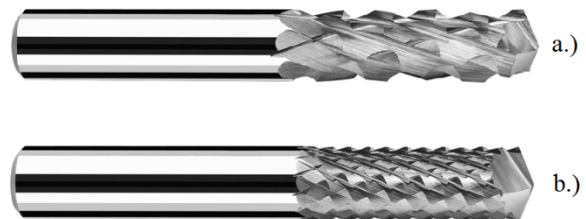


Fig. 1 a.) Fraisa 20340.450 and b.) Fraisa 20360.450 compression end mills

In a previous study Lacalle et al. [10] researched these tool's wear, and wear dependent efficiency. Despite this interest, the investigation of optimized machining parameters for these special tools is still neglected.

The main objective of the present study was to reach a deeper understanding on how basic machining factors (tool and cutting width) influence the optimization parameters (cutting force and surface roughness), in cases where compression end mills were applied.

## 2 EXPERIMENTAL SETUP AND CUTTING CONDITIONS

### 2.1 Environment

The machining experiments were carried out on a Kondia B640 milling machine centre. A KISTLER 9257BA type load cell was used for the measurement of the cutting force, likewise a Mahr Federal Pocket Surf IV instrument for surface roughness. A Fraisa 20340.450 (referred as coarse tool) and a Fraisa 20360.450 (referred as medium tool) compression end mills (Fig. 3) were used with climb milling technology.

The examined UD-CFRP block was fixed with two clamps as can be seen in Fig. 2. Two microscopes were placed in the workspace for the detection of tool wear.

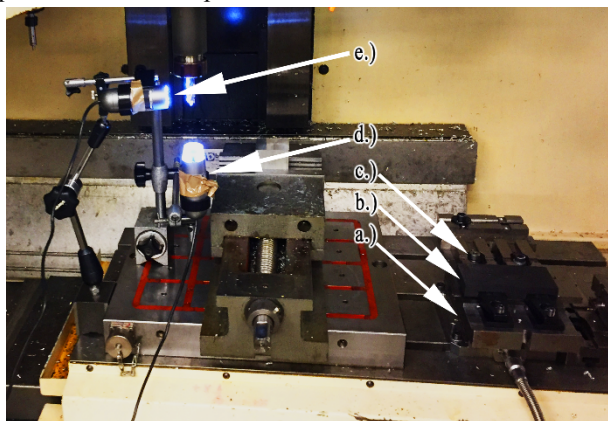


Fig. 2 Experimental setup. a) UD-CFRP specimen; b) fixture c) KISTLER load cell d.), e.) digital microscopes

Milling experiments were designed using central composite inscribed (CCI) design. Cutting with and feed rate were chosen as factors in order to analyse their influence on the optimisation parameters: cutting force and surface roughness. Other process parameters, such as revolutions per minute ( $n=3185$  1/min), milling style (down milling) and depth of cut ( $a_p=18$  mm), as well as extreme values for the CCI design were fixed based on previous works [11], [12] and suggestions of tool manufacturers.

During the experiments, workpiece was face milled. The edges of the cutting tool are captured in original state, to be used later as a control picture. The three dimensional cutting force data were collected at 8000 Hz frequency. During the machining the abrasive chips were vacuumed. After the machining, images of the machined surface were taken by a Dino-lite AD7013MZT digital microscope. Thereafter the surface roughness was measured perpendicularly to the toolpath five times along the cut. In the meantime photos of the tool were taken for subsequent comparison.

### 3 RESULTS AND DISCUSSION

Thirteen experiments were carried out for each tool. The randomised experiment design tables were calculated with MiniTab 17. The results for each experiment are shown in Table 1 and Table 2

Using response surface methodology (RSM), a quadratic polynomial model on data was developed. The second-degree formula used in this study is expressed by Eq.(1).

$$y = b_0 + \sum_{i=1}^n b_i x_i + \sum_{i=1}^n b_{ii} x_{ii}^2 + \sum_{i=1}^{n-1} \sum_{j=i+1}^n b_{ij} x_i x_j + \delta \quad (1)$$

, where  $y$  is the optimisation parameter,  $b$  marks constant multipliers,  $x$  marks the factors, and  $n$  is the number of factors, while  $\delta$  is the error-factor.

#### 3.1 Cutting force

The cutting force data were interfered with distortion such as machine noise from the milling centre. The data has been low-pass filtered with discrete Fourier transformation (DFT). The signals which belong to higher frequency

domains has been removed. The results shown in Table 1 and Table 2 are the maximum force values given by the filtered data set. The resultant maximum force is calculated as expressed by Eq.(2).

$$F_{momentary} = \max_{j:1 \in n} \left\{ \sqrt{F_{x,j}^2 + F_{y,j}^2 + F_{z,j}^2} \right\} \quad (2)$$

, where  $F_{momentary}$  (N) is the momentary cutting force,  $F_x$  (N) is the radial,  $F_y$  (N) is the feed-directional and  $F_z$  (N) is the axial (passiv) component of the cutting force. As can be seen on the Fig. 4, on both tool's main effect diagrams, the feed rate has the most significant effect on the cutting force, followed by the cutting width. Furthermore, both factor increases the cutting force.

Analysis of variance (ANOVA) and interaction plots confirm that the two analysed factors have no considerable interaction terms. The response surfaces for the tools are shown in the Fig. 3. Both the increase of feed rate and cutting width results in rise of the cutting force. It can be seen that in each case, the maximum cutting force is awaked at maximum factor levels ( $v_f=1200$  mm/min and  $a_e=5$  mm).

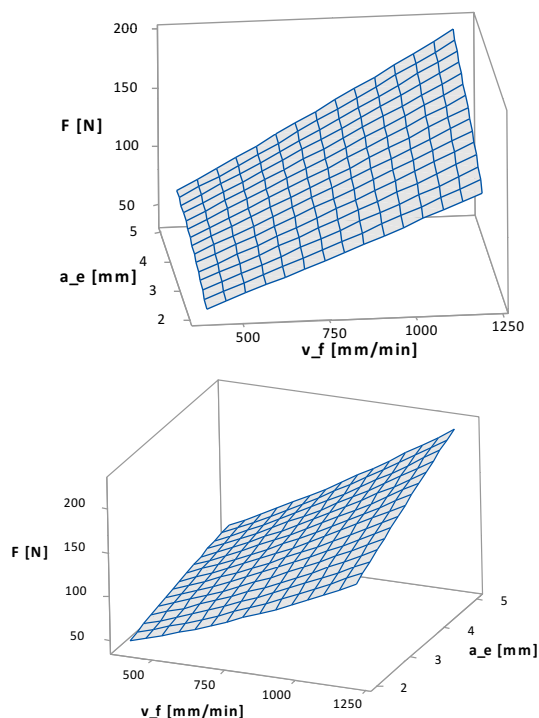


Fig. 3 Response surfaces of cutting force for tools 20340.450 and 20360.450, respectively.

**Table 1** Experimental setting for the Fraisa 20340.450 tool, with parameters generated by CCI design, and averaged  $Ra$  values, and the resultant  $F$  force

Nr.	Factors		Results				
	$v_f$ (mm/min)	$a_e$ (mm)	$Ra$ ( $\mu$ m)	$F_x$ (N)	$F_y$ (N)	$F_z$ (N)	$F$ (N)
1	800	3.50	2.56	68.28	74.44	37.03	106.89
2	517	4.56	2.94	60.71	42.69	30.80	79.47
3	800	2.00	3.21	46.28	62.90	28.66	83.14
4	800	5.00	3.19	100.62	70.54	50.37	131.52
5	1083	4.56	2.67	120.53	98.34	65.27	166.09
6	400	3.50	1.73	43.34	33.75	21.73	57.58
7	1200	3.50	2.59	103.57	118.47	58.50	166.53
8	800	3.50	2.45	72.80	74.55	40.09	110.96
9	1083	2.44	2.81	72.00	97.25	44.94	126.88
10	800	3.50	2.39	76.34	76.31	43.24	112.87
11	800	3.50	2.37	72.87	74.15	38.67	109.77
12	517	2.44	2.40	39.76	40.63	20.38	59.38
13	800	3.50	3.06	73.52	73.77	38.08	109.05

**Table 2** Experimental setting for the Fraisa 20360.450 tool, with parameters generated by CCI design, and averaged  $Ra$  values, and the resultant  $F$  force

Nr.	Factors		Results				
	$v_f$ (mm/min)	$a_e$ (mm)	$Ra$ ( $\mu$ m)	$F_x$ (N)	$F_y$ (N)	$F_z$ (N)	$F$ (N)
1	400	3.50	2.04	45.15	39.18	25.55	63.60
2	800	2.00	1.44	47.56	66.36	36.93	88.94
3	517	4.56	2.32	72.66	44.70	37.39	92.65
4	800	3.50	2.25	76.91	75.38	48.05	116.16
5	517	2.44	2.27	43.63	43.32	26.79	66.42
6	800	5.00	2.37	117.60	67.04	62.90	147.09
7	800	3.50	1.76	81.73	74.92	52.70	121.11
8	800	3.50	1.68	82.27	75.69	53.41	121.89
9	800	3.50	1.85	83.30	74.98	54.89	122.91
10	1083	2.44	2.38	84.54	99.07	61.18	141.52
11	1200	3.50	1.70	127.71	118.08	85.62	188.29
12	1083	4.56	1.73	140.59	101.59	85.51	190.25
13	800	3.50	1.80	83.25	75.18	52.06	121.73

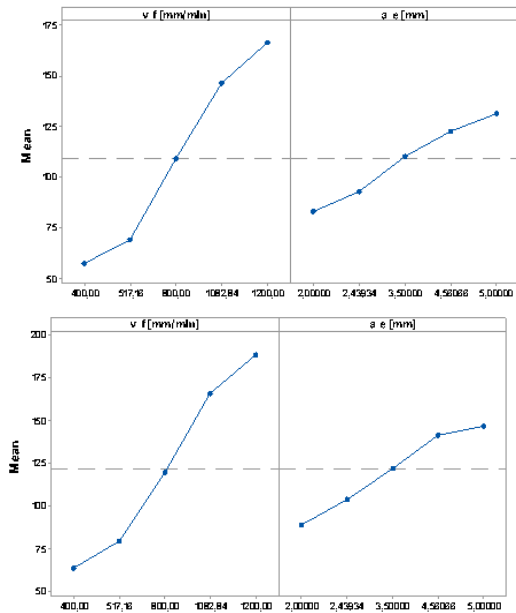


Fig. 4 Main effect diagrams of cutting force for tools 20340.450 and 20360.450, as is

The developed models are shown by Eq. (3) and (4). According to the models and the response surfaces, the compression end mill with coarse tooth is affected by up to 20% smaller force. The possible reason if this is, that the sufficient energy for starting chip splitting is higher than the amount of energy needed for maintaining a cut. The tool with fewer edges starts new chips more often, in other words transmit more energy towards the workpiece, hence generates greater forces.

$$F = -20.8 + 0.0677v_f + 13.02a_e + 0.000008v_f^2 - 1.531a_e^2 + 0.01593v_f a_e \quad (3)$$

$$F = -5.8 + 0.0332v_f + 10.93a_e + 0.000035v_f^2 - 1.057a_e^2 + 0.01875v_f a_e \quad (4)$$

Moreover,  $F_z$  values are considerably lower than the other two components of the cutting force. It caused by the tool geometry in purpose. In this direction, the generated force on the neighbouring edges are opposed, as shown on the Fig. 5, thus resulting a smaller resultant force.

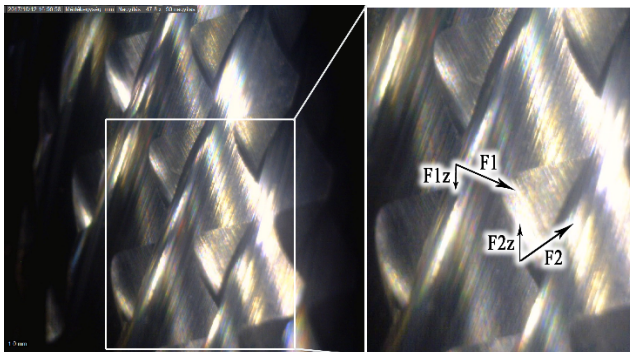


Fig. 5 Vector sum for z directional local cutting forces

### 3.2 Surface roughness

The surface roughness was measured five times along the surface, perpendicularly the toolpath, then average

surface roughness ( $Ra$ ), roughness depth ( $Rz$ ) and their proportion ( $Rz/Ra$ ) were calculated. The collected data was filtered for deviant values. The examined values were obtained based on the the average of the five points. The response surfaces can be seen in the Fig. 6. It can be observed from the main effect diagrams, shown on the Fig. 7, that both factors have significant impact on the measured  $Ra$  values. Although, for the coarse tool the data is inconsistent. This was most likely caused by the amount of uncut fibres along the surface, which is a common machining defect for CFRP [9], [13]. In the case of the coarse tool, the response surface forms a saddle surface. Based on the quadratic equation fitted on the data set, the optimal cutting width for a given feed rate, is 3.03 mm. This can be used for getting smoother surface along the joining points of the finished component.

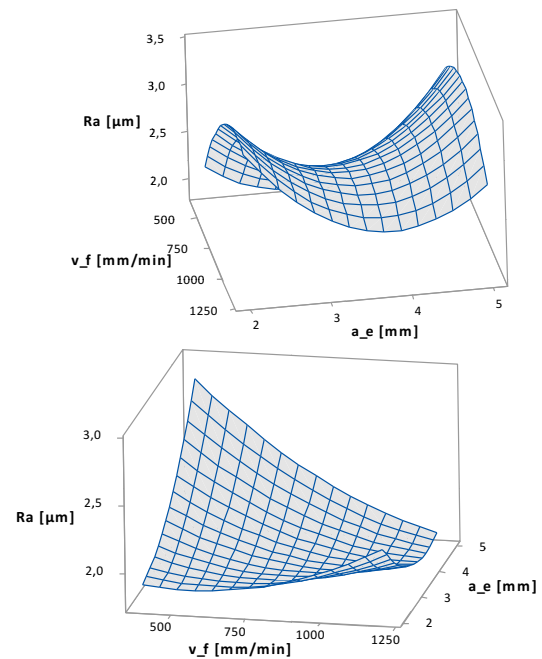


Fig. 6 Response surfaces of average surface roughness ( $Ra$ ) for tools 20340.450 and 20360.450, respectively

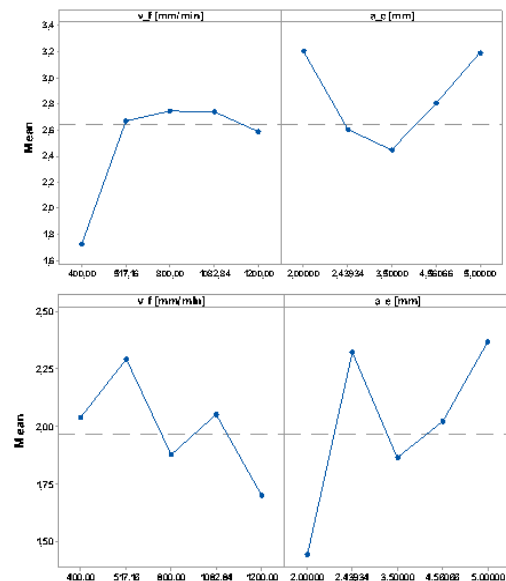


Fig. 7 Main effects diagram of average surface roughness for tools 20340.450 and 20360.450, respectively

As mentioned before, the amount of uncut fibres is a key parameter during machining of CFRP. We can get broader picture of this amount by inspecting the  $Rz/Ra$  ratio. Average surface roughness ( $Ra$ ) is calculated as the arithmetical average value of all absolute differences from the centre line. This method tends to pay little attention for short high peaks, such as these fibres, or short deep valleys, like delamination on the surface. Roughness depth ( $Rz$ ) is measured as the average distance from the highest peak to the lowest valley on five sampling lengths.  $Rz/Ra$  ratio gives us a proper value to represent the quantity of typical CFRP surface defects created during milling [7].

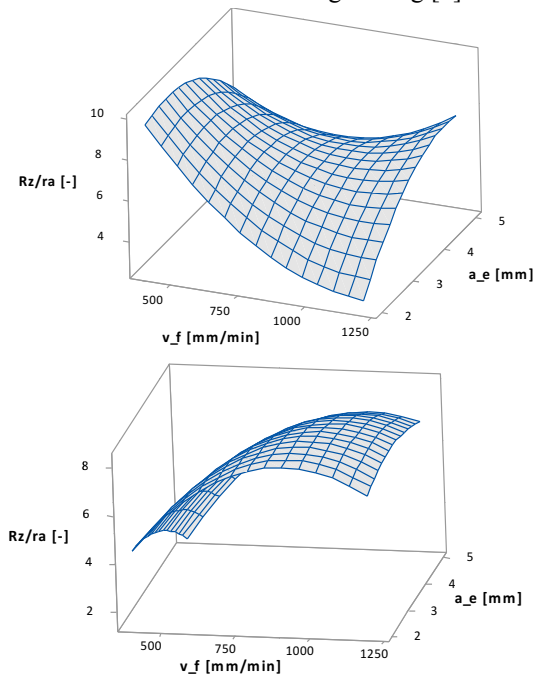


Fig. 8 Response surfaces of  $Ra/Rz$  ratio for tools 20340.450 and 20360.450, as is

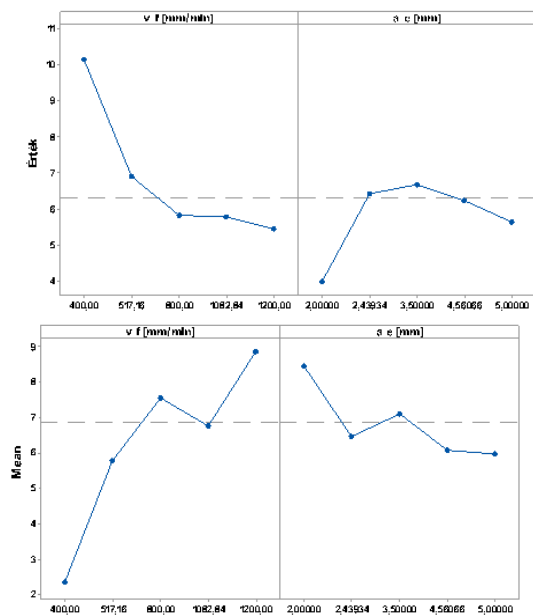


Fig. 9 Main effect diagram of  $Ra/Rz$  ratio for tools 20340.450 and 20360.450, as is

The response surfaces of the  $Rz/Ra$  ration are shown in the Fig. 8. On the basis of these and the ANOVA table, it's

clear that the feed rate has by far more significant effect on the optimization parameter. Increase of feed rate results in the decrease of this parameter. Therefore, it is advisable to use high feed near the joining points of the finished component.

#### 4 CONCLUSIONS

In the present study, milling experiments were carried out in uni-directional CFRP using compression end mills in order to analyse and optimise process parameters. According to the present study, the following conclusions can be drawn:

- In the case of both compression end mills, both analysed factors (feed rate and cutting width) increase the cutting force, moreover the feed rate has the most significant effect on the cutting force, followed by the cutting width.
- RSM models were developed to analyse the influence of the factors on the cutting force. Cutting force were observably greater in the case of the compression tool with coarse tooth. This was possibly caused by the higher energy need of new chip formation.
- $Fz$  (passiv) force component values are significantly lower than the other two components of the cutting force. It's caused by the tool geometry. The axial forces on the neighbouring edges are opposed, therefore these add up to smaller resultant passiv force.
- Both factors have significant impact on the measured  $Ra$  values. For the compression end mill with coarse tooth the optimal cutting width for any given feed rate, is 3.03 mm.
- Feed rate has by far more significant effect on the  $Rz/Ra$  ratio than the cutting width. Increase of feed rate results in the decrease of this parameter. Therefore, use of high feed rates near the joining points during the finishing of the component leads to better surface quality, therefore better bonding.

#### ACKNOWLEDGEMENT

The authors would like to acknowledge the support provided by the CEEPUS III HR 0108 project. This research was partly supported by the EU H2020-WIDESPREAD-01-2016-2017-TeamingPhase2-739592 project "Centre of Excellence in Production Informatics and Control" (EPIC). Furthermore, the authors acknowledge to prof. Gyula MÁTYÁSI and to the BSc students Csenge BÉKY, Kristóf SZOBODEK and Bertalan ZACHER for their participation in the experimental work.

#### REFERENCES

- [1] M. Saleem, L. Toubal, R. Zitoune, and H. Bougherara, 'Investigating the effect of machining processes on the mechanical behavior of composite plates with circular holes', *Compos. Part Appl. Sci. Manuf.*, vol. 55, no. Supplement C, pp. 169–177, 2013.
- [2] C. Soutis, 'Fibre reinforced composites in aircraft construction', *Prog. Aerosp. Sci.*, vol. 41, no. 2, pp. 143–151, 2005.
- [3] C. Soutis, 'Carbon fiber reinforced plastics in aircraft construction', *Mater. Sci. Eng. A*, vol. 412, no. 1, pp. 171–176, 2005.
- [4] R. Zitoune, V. Krishnaraj, and F. Collombet, 'Study of drilling of composite material and aluminium stack', *Compos. Struct.*, vol. 92, no. 5, pp. 1246–1255, Apr. 2010.
- [5] L. Sorrentino, S. Turchetta, and C. Bellini, 'In process monitoring of cutting temperature during the drilling of FRP laminate', *Compos. Struct.*, vol. 168, no. Supplement C, pp. 549–561, May 2017.
- [6] R. Voss, M. Henerichs, and F. Kuster, 'Comparison of conventional drilling and orbital drilling in machining carbon fibre reinforced plastics (CFRP)', *CIRP Ann.*, vol. 65, no. 1, pp. 137–140, 2016.
- [7] N. Geier and T. Szalay, 'Optimisation of process parameters for the orbital and conventional drilling of uni-directional carbon fibre-reinforced polymers (UD-CFRP)', *Measurement*, vol. 110, no. Supplement C, pp. 319–334, 2017.
- [8] H. Wang, J. Sun, J. Li, L. Lu, and N. Li, 'Evaluation of cutting force and cutting temperature in milling carbon fiber-reinforced polymer composites', *Int. J. Adv. Manuf. Technol.*, vol. 82, no. 9–12, pp. 1517–1525, Feb. 2016.
- [9] M. K. N. Khairushshima, A. K. N. Aqella, and I. S. S. Sharifah, 'Optimization of Milling Carbon Fibre Reinforced Plastic Using RSM', *Procedia Eng.*, vol. 184, no. Supplement C, pp. 518–528, 2017.
- [10] L. Lacalle, A. Lamikiz, F. Campa, A. FDZ. Valdivielso, and I. Etxeberria, 'Design and Test of a Multitooth Tool for CFRP Milling', *J. Compos. Mater. - J COMPOS MATER*, vol. 43, pp. 3275–3290, 2009.
- [11] N. Geier, 'Machinability study of uni-directional CFRP using fractional factorial design', *Bp. Univ. Technol. Econ. TDK Study*, 2015.
- [12] Norbert Geier and Gyula Matyasi, 'Machinability Study of Unidirectional CFRP Using Central Composite Design of Experiments', *Óbuda Univ. E-Bull.*, vol. Vol. 6, No. 1, 2016, 2016.
- [13] R. Voss, L. Seeholzer, F. Kuster, and K. Wegener, 'Influence of fibre orientation, tool geometry and process parameters on surface quality in milling of CFRP', *CIRP J. Manuf. Sci. Technol.*, vol. 18, no. Supplement C, pp. 75–91, 2017.